

Distribution of Dual Additives Enables Efficient Semi-Transparent Layer-By-Layer Architecture of Organic Solar Cells

Ji Youn Kim,^a Sung Jae Jeon,^a Hyoung Seok Lee,^a Yong Woon Han,^a Ye Chan Kim,^a Nam Gyu Yang,^a Gang Wook Kim,^a Eun Mi Jang,^a Ji Hyeon Kim,^a and Doo Kyung Moon^{*a}

^a Department of Chemical Engineering Konkuk University, Seoul 05029, Republic of Korea

* Corresponding author

Experiment

Materials: PM6(FPy=0.2) used as a donor was synthesized in our group by following reference.¹ PM6, D18, L8-BO, BTP-eC9 and PDINN were purchased from Derthon Optoelectronic Materials Science Technology CO. Ltd. (China). 1-Chloronaphthalene (CN, 85%) used as the solvent additive was from TCI. Poly(dimethylsiloxane-co-diphenylsiloxane), dihydroxy terminated (PDMDP) used as the polymer additive, chloroform (CF, 99.8%), chlorobenzene (CB, 99.8%), and methanol (MeOH, 99.8%) were purchased from Sigma Aldrich (USA). Poly(3,4-ethylenedioxythiophene):polystyrenesulfonate (PEDOT:PSS; Clevios P VP Al 4083) from Heraeus. Indium tin oxide (ITO) glass substrate was purchased from AMG Korea.

Preparation of dual additives solution: The CN and PDMDP were used as additives into the solvent, CB. For CN and PDMDP, the optimized amount of 0.5 vol% (5 μL was added into the solution of CB with 1.0 mL) was introduced into device 1 and device 2, respectively. For CN + PDMDP, the ratio of CN and PDMDP is 1:0.25 (v/v; 500:125 (μL)), and were mixed in glovebox. After mixing properly, the amount of 0.625 vol% (6.25 μL was added into the solution of CB with 1.0 mL) used as dual additives. For (H) CN + PDMDP, it was same procedure as the previously dual additives and then performed the heating process for dissolving them completely at 150 °C (7 min).²

Active layer solution: The BHJ devices were processed with PM6(FPy=0.2):BTP-eC9 = 1:1.2 (22mg mL⁻¹, w/w) dissolved in CB (CN, 0.5%) of device 1 or CB (PDMDP, 0.5%) of device 2. The BHJ devices based on dual additives were processed with the same active materials which dissolved in CB (CN + PDMDP, 0.625% v/v) of device 3 or CB ((H) CN + PDMDP, 0.625% v/v) of device 4. For the universal test of different BHJ-based devices with dual additives, two photovoltaic systems (PM6:L8-BO = 1:1 (15 mg mL⁻¹, w/w) and D18:BTP-eC9 = 1:1.6 (11.7 mg mL⁻¹, w/w)) were dissolved in CF. The next following are the fabrication details of LBL devices. First, the PM6(FPy=0.2) / BTP-eC9-based devices, PM6(FPy=0.2) was dissolved in CB at a concentration of 12 mg mL⁻¹. The acceptor, BTP-eC9, was dissolved in CF with 1,8-diiodooctane (DIO) 0.25 vol% at a concentration of 10 mg mL⁻¹. For the universal test of LBL-based PM6/L8-BO devices with dual additives, the concentrations of PM6 and L8-BO are used with 10 mg mL⁻¹ and 8 mg mL⁻¹, respectively. Meanwhile, for LBL-based D18/BTP-eC9 devices with dual additives, the concentrations of D18 and BTP-eC9 are used with 7 mg/mL and 10 mg/mL, respectively. For device 1, as the solvent additive, CN (0.5% v/v) was added to the donor solution. For device 2, as the polymer additive, PDMDP (0.5% v/v) was added to the donor solution. The dual additives of CN and PDMDP were added to the donor solution of device 3 (CN + PDMDP, 0.625% v/v) or of device 4 ((H) CN + PDMDP, 0.625% v/v), respectively. The other details are the same as PM6(FPy=0.2) / BTP-eC9 -based devices. All the additive amounts were optimized for manipulating the morphology. All solutions were preheated on the hotplate at 60 °C.

Device Fabrication and materials: All OSCs were fabricated in a conventional structure with ITO/PEDOT:PSS/Active layers/PDINN/Ag. The patterned ITO glass substrates were treated with ultrasonication cleaning by detergent, iso-propanol and de-ionized water in order. Then, ITO substrates were blown dry with a nitrogen gun and treated with UV-ozone (UVO) cleaner (Ahtech LTS AH1700) for 30 min. The PEDOT:PSS was spin-coated (4000 rpm, 30 s) onto ITO substrate and annealed at 110 °C for 10 min in the ambient condition. Afterward, the PEDOT:PSS substrates were transferred to the glovebox filled with high-purity

nitrogen. For the BHJ films, PM6(FPy=0.2):BTP-eC9 blends were spin-coated (3,500-4,000 rpm, 30 s) onto the PEDOT:PSS substrates to form the active layers of about 100 nm thickness. For LBL films, donor solutions were first spin-casted at a rate of 2500-3500 rpm onto the PEDOT:PSS substrates, and then acceptor solutions were spin-casted at a rate of 3500-4000 rpm onto the donor layer, directly. After that, active layer films were annealed at 100 °C for 10 min. The prepared PDINN solution (1 mg mL⁻¹ MeOH), was spin-coated (3000 rpm, 30s) onto the active layer substrates. Finally, 100 or 12 nm Ag was deposited 1 Å s⁻¹ by the thermal evaporation (10⁻⁷ torr vacuum) as top electrode. The active area is 4.0 mm² with a mask.

Device characterization: The short-circuit current density-voltage (*J-V*) characteristics were measured by Keithley 2400 source meter. AM 1.5 G irradiation at 100 mW cm⁻² was provided by a solar simulator (Oriel, 1,000 W). The external quantum efficiency (EQE) spectra were measured with Polaronix K3100 IPCE measurement system (Mc science, Korea) in the ambient atmosphere. The absorption and transmittance (T) spectra are conducted by the ultraviolet-visible (UV-Vis) spectrometer (Agilent 8453). Reflection (R) spectra were collected by QEX7, reflectance measuring mode. The electrostatic potential (ESP) surfaces of CN and PDMDP were calculated by using the density functional theory as b3lyp/6-31g(d) functions of Gaussian 09. For analyzing the orientation/crystallinity, morphology, and depth profile of active layers, grazing incidence wide angle X-ray scattering (GIWAXS), atomic force microscope (AFM), field emission scanning electron microscope analysis (FE-SEM), and time-of-flight secondary ion mass spectrometry (ToF-SIMS) were used, respectively. The GIWAXS were conducted using PLS-II 9A U-SAXS beamline, Pohang Accelerator Laboratory in Korea. The AFM characterization was scanned by PSIA XE-100 using a non-contact mode, in which the AFM images have the *x*-axis and *y*-axis scales of 10 μm × 10 μm. The FE-SEM was performed with a JSM-7600F (Jeol). The ToF-SIMS characterization was performed using a TOF.SIMS 5 instrument, Korea Institute of Science and Technology (KIST) in Korea (ION-TOF Münster, Germany), where a 3 keV Cs⁺ ion beam was used for erosion and a 30 keV Bi³⁺ pulsed primary ion beam was used for the analysis. The film sample was coated on ITO glass using the same processing conditions as those for device fabrication. The electron and hole mobilities were calculated using the space charge limited current (SCLC) method equation: $J = (9/8)\epsilon_r\epsilon_0\mu(V^2/d^3)$ (μ : charge carrier mobility, ϵ_r : dielectric constants, ϵ_0 : the of free-space and the permittivity, V : applied voltage, d : thickness)^{1,3} The hole-only and electron-only devices were fabricated with structures of ITO/PEDOT:PSS(AI 4083)/active layer/PEDOT:PSS(HTL solar)/Ag and ITO/ZnO sol-gel/active layer/PDINN/Ag, respectively.

Table S1 Photovoltaic parameters of the optimized LBL-OSC devices with respect to (H) CN + PDMDP ratios.

(H) CN + PDMDP	J_{SC} [mA cm ⁻²]	V_{OC} [V]	FF [%]	PCE ^a [%]
0.05	24.7 (24.50 ± 0.19)	0.838 (0.836 ± 0.001)	74.60 (74.45 ± 0.15)	15.50 (15.42 ± 0.07)
0.1	25.1 (24.95 ± 0.12)	0.838 (0.836 ± 0.002)	75.20 (75.08 ± 0.12)	15.80 (15.69 ± 0.11)
0.5	25.3 (25.10 ± 0.18)	0.838 (0.836 ± 0.002)	75.30 (75.12 ± 0.17)	16.00 (15.90 ± 0.08)
0.625	26.1 (25.95 ± 0.12)	0.831 (0.830 ± 0.001)	76.24 (76.18 ± 0.06)	16.51 (16.42 ± 0.07)

^a Champion value and average values (in parenthesis) are obtained from 10 devices.

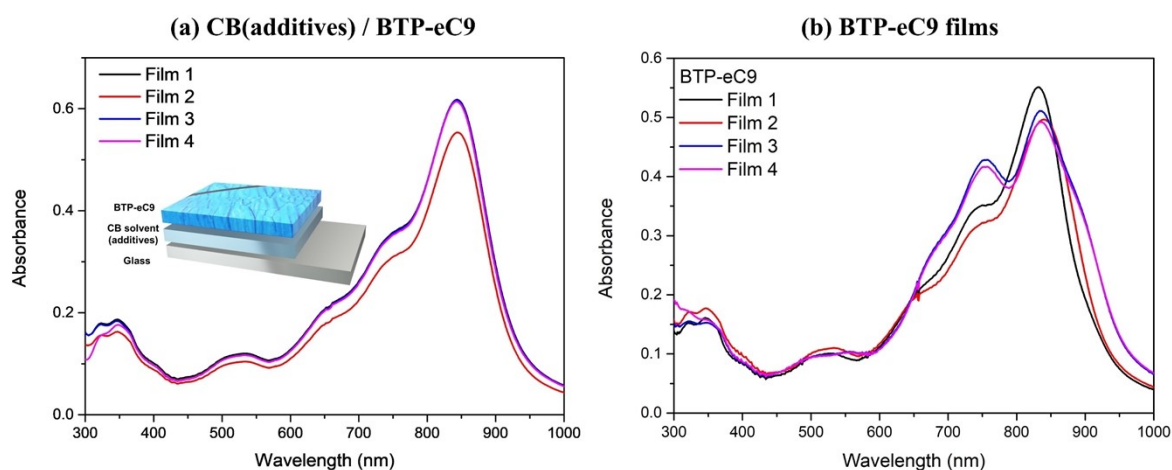


Fig. S1 UV-Vis spectra of (a) CB(additive(s))/BTP-eC9 films and (b) neat BTP-eC9 films with respect to the additive: CN (film 1), PDMDP (film 2), CN + PDMDP (film 3), and (H) CN + PDMDP (film 4).

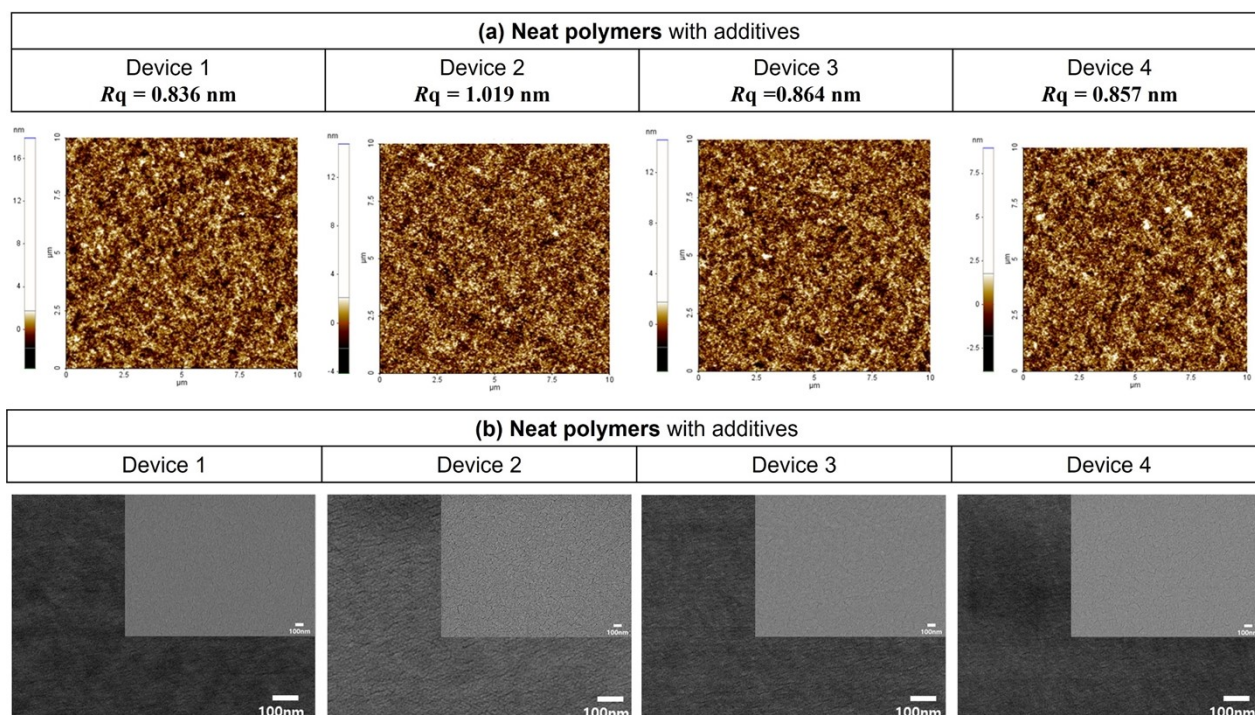


Fig. S2 (a) AFM height and (b) SEM images of neat polymer films with respect to the additive.

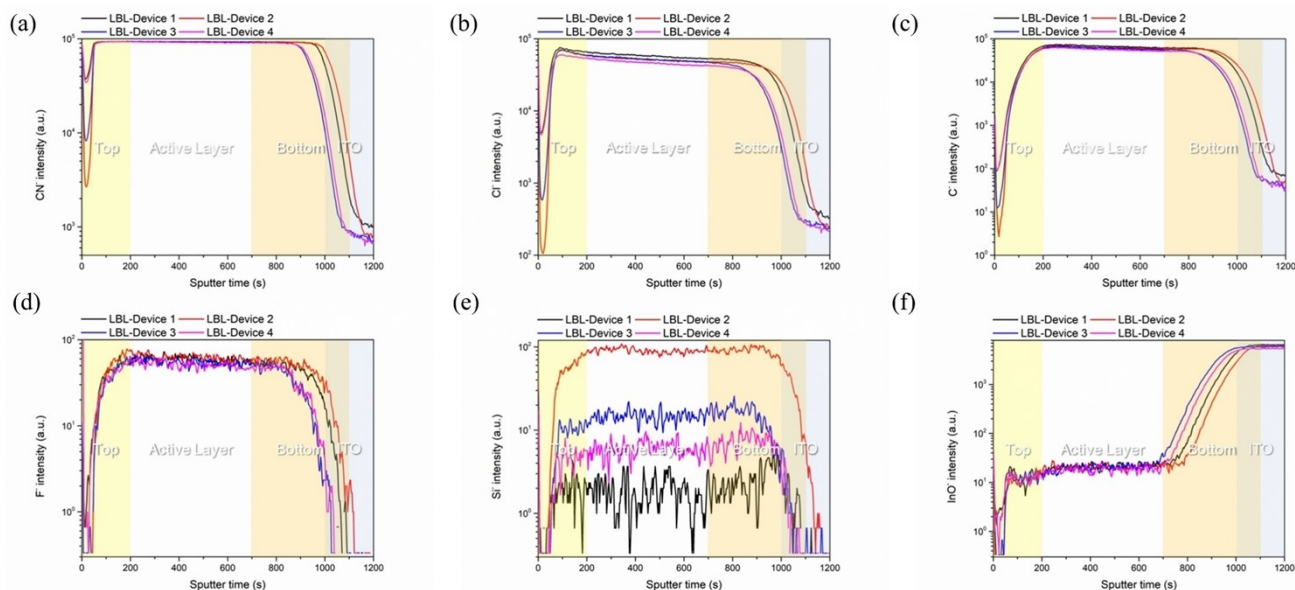


Fig. S3 ToF-SIMS depth profiles of LBL-processed blend films coated on ITO glass with respect to the additive: Ion intensity of (a) CN; (b) Cl; (c) C; (d) F; (e) Si; and (f) InO.

Table S2 Detailed parameters from GIWAXS profiles of neat polymer films with respect to the additive.

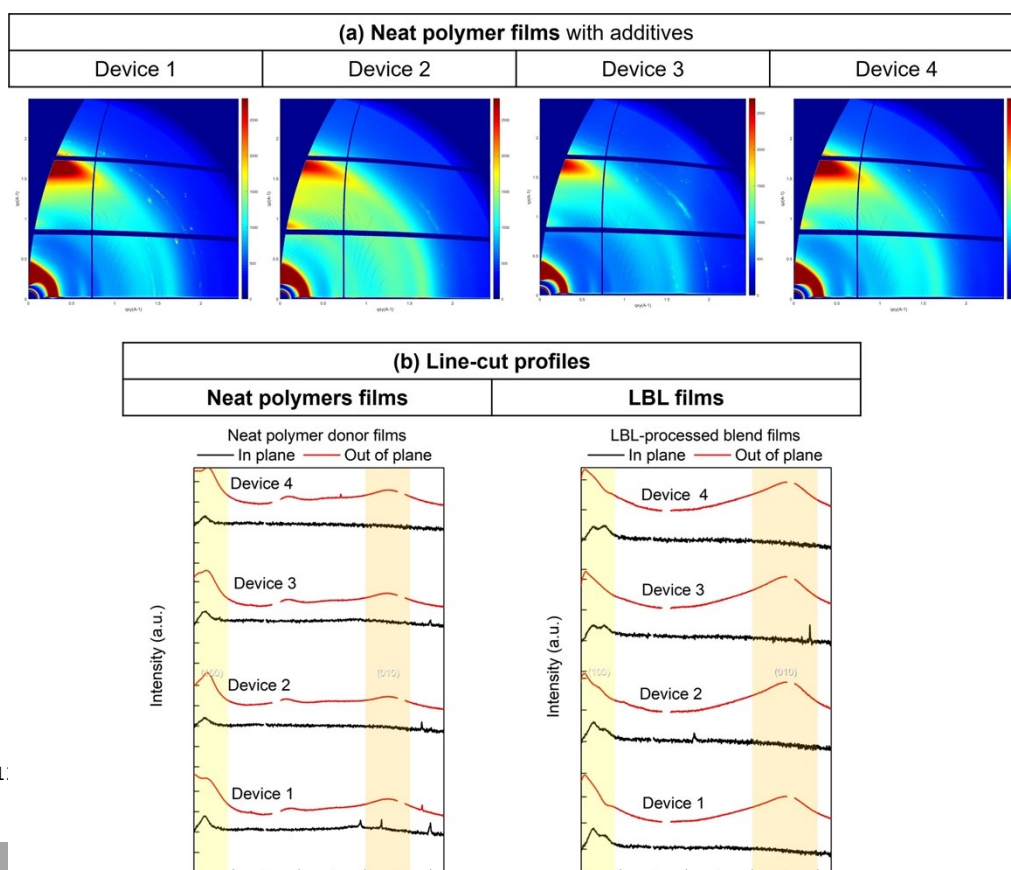


Fig. S4 (a) GIWAXS patterns of neat polymer films with respect to the additive. (b) line-cut profiles of GIWAXS patterns of both neat polymer and LBL-processed blend films with respect to the additive.

	Orientation	q (\AA^{-1})	d -spacing (\AA)	FWHM (\AA^{-1})	CCL (\AA)
PM6(FPy=0.2) CN	(100)	0.284	22.139	0.131	43.006
	(300)	0.932	6.744	0.080	70.828
	(010)	1.678	3.744	0.205	27.554
PM6(FPy=0.2) PDMDP	(100)	0.299	21.042	0.078	72.769
	(300)	0.903	6.958	0.118	47.927
	(010)	1.676	3.749	0.174	32.570
PM6(FPy=0.2) CN + PDMDP	(100)	0.295	21.306	0.106	53.207
	(300)	0.921	6.823	0.190	29.691
	(010)	1.669	3.765	0.199	28.375
PM6(FPy=0.2) (H) CN + PDMDP	(100)	0.308	20.400	0.084	67.225
	(300)	0.921	6.822	0.114	49.648
	(010)	1.686	3.727	0.199	28.351

	Orientation	q (\AA^{-1})	d -spacing (\AA)	FWHM (\AA^{-1})	CCL (\AA)
LBL-Blend CN	(100)	0.230	27.318	0.097	58.503
	(010)	1.758	3.575	0.249	22.703
LBL-Blend PDMDP	(100)	0.226	27.777	0.121	46.645
	(010)	1.759	3.572	0.274	20.652
LBL-Blend CN + PDMDP	(100)	0.234	26.897	0.185	30.537
	(010)	1.754	3.581	0.246	23.014
LBL-Blend (H) CN + PDMDP	(100)	0.226	27.777	0.178	31.776
	(010)	1.762	3.564	0.231	24.440

Table S3 Detailed parameters from GIWAXS profiles of LBL-processed blend films with respect to the additive.

	α	kT/q	μ_e [$\text{cm}^2 \text{V}^{-1} \text{s}^{-1}$]	μ_h [$\text{cm}^2 \text{V}^{-1} \text{s}^{-1}$]	μ_e/μ_h
Device 1	1.0347	1.110	7.28×10^{-4}	3.89×10^{-4}	1.871
Device 2	1.0381	1.115	4.81×10^{-4}	3.34×10^{-4}	1.440
Device 3	1.0367	1.122	6.59×10^{-4}	4.99×10^{-4}	1.321
Device 4	1.0343	1.107	6.74×10^{-4}	6.09×10^{-4}	1.107

Table S4 Detailed parameters of Light intensity dependence (J_{sc} and V_{oc}) and SCLC for the optimized OSC devices based on LBL process.

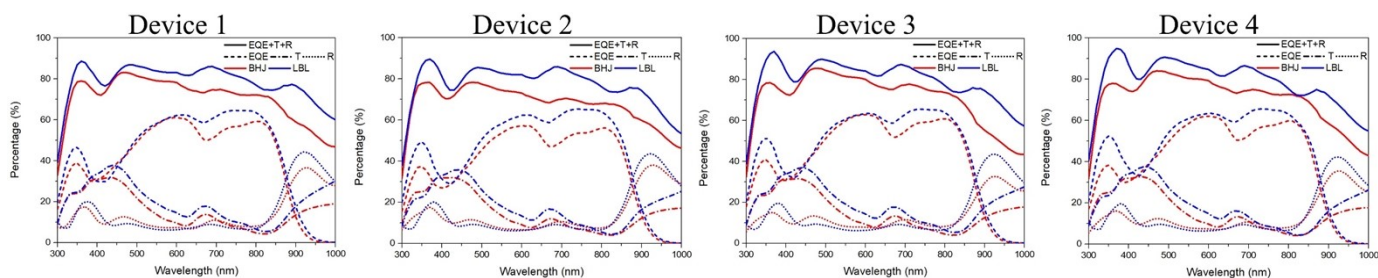


Fig. S5 EQE, T, R, and EQE + T + R curves of the optimized ST-OSC devices based on BHJ and LBL processes with respect to the additive: BHJ (red) and LBL devices (blue).

Table S5 Photovoltaic parameters of the different active materials based on BHJ and LBL processes with respect to the additive.

Active layer (BHJ and LBL)		J_{sc} [mA cm ⁻²]	V_{oc} [V]	FF [%]	PCE ^a [%]
PM6:L8-BO (BHJ-OSC devices)	Device 1	23.8 (23.4 ± 0.4)	0.866 (0.867 ± 0.001)	79.71 (79.80 ± 0.09)	16.49 (16.22 ± 0.27)
	Device 3	24.2 (23.8 ± 0.4)	0.865 (0.864 ± 0.001)	79.55 (79.49 ± 0.06)	16.65 (16.36 ± 0.29)
	Device 4	23.9 (23.3 ± 0.4)	0.865 (0.866 ± 0.001)	79.18 (78.97 ± 0.21)	16.34 (16.03 ± 0.31)
PM6/L8-BO (LBL-OSC devices)	Device 1	21.3 (21.2 ± 0.1)	0.867 (0.869 ± 0.002)	79.43 (79.60 ± 0.17)	14.67 (14.58 ± 0.09)
	Device 3	21.7 (21.4 ± 0.3)	0.866 (0.866 ± 0.001)	79.42 (79.50 ± 0.08)	14.90 (14.77 ± 0.13)
	Device 4	21.3 (21.1 ± 0.2)	0.865 (0.867 ± 0.002)	79.84 (79.75 ± 0.09)	14.68 (14.56 ± 0.12)
D18:BTP-eC9 (BHJ-OSC devices)	Device 1	24.5 (24.1 ± 0.4)	0.845 (0.847 ± 0.002)	76.33 (76.91 ± 0.58)	15.82 (15.54 ± 0.21)
	Device 3	22.8 (22.2 ± 0.6)	0.845 (0.838 ± 0.007)	69.27 (69.00 ± 0.27)	13.33 (13.00 ± 0.33)
	Device 4	24.9 (25.1 ± 0.2)	0.867 (0.862 ± 0.005)	72.31 (72.00 ± 0.31)	15.61 (15.40 ± 0.21)
D18/BTP-eC9 (LBL-OSC devices)	Device 1	24.9 (24.4 ± 0.5)	0.836 (0.834 ± 0.002)	78.92 (78.65 ± 0.27)	16.40 (16.10 ± 0.30)
	Device 3	25.4 (24.8 ± 0.6)	0.836 (0.835 ± 0.001)	78.16 (77.91 ± 0.25)	16.59 (16.30 ± 0.29)
	Device 4	24.4 (24.1 ± 0.3)	0.837 (0.837 ± 0.001)	77.90 (77.74 ± 0.16)	15.99 (15.73 ± 0.26)

^a Champion value and average values (in parenthesis) are obtained from 10 devices.

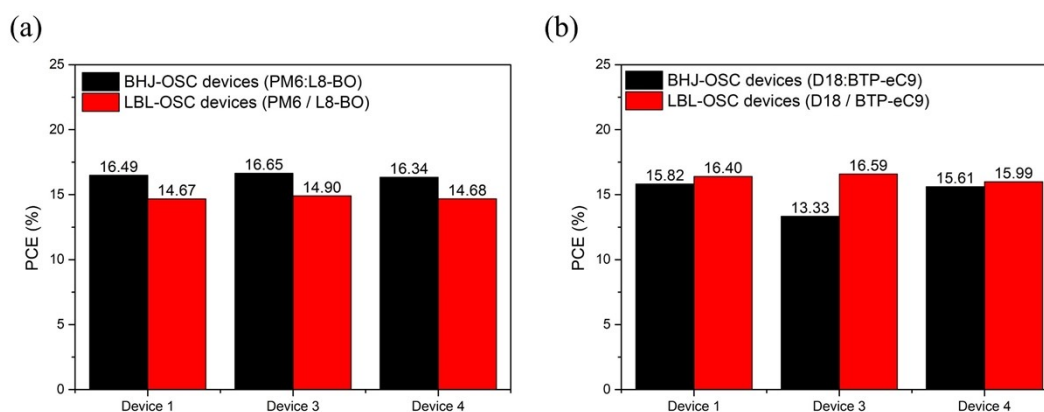


Fig. S6 Photovoltaic results of the different active materials based on BHJ and LBL processes with respect to the additive: (a) PM6:L8-BO and PM6/L8-BO, (b) D18:BTP-eC9 and D18/BTP-eC9.

References

- 1 S. J. Jeon, N. G. Yang, J. Y. Kim, Y. C. Kim, H. S. Lee and D. K. Moon, *Small*, 2023, **19**, 2301803
- 2 S. Morariu, C. E. Brunchi, M. Cazacu and M. Bercea, *J. Chem. Eng. Data*, 2011, **56**, 1468–1475.
- 3 Y. W. Han, S. J. Jeon, H. S. Lee, H. Park, K. S. Kim, H. Lee and D. K. Moon, *Adv. Energy Mater.*, 2019, **9**, 1902065.